Journal of Comparative Physiology A
https://doi.org/10.1007/s00359-024-01712-7

RESEARCH

Expression of proteins supporting visual function in heterobranch gastropods

Ryota Matsuo[1] · Haeri Kwon[1] · Kiyotaka Takishita[1] · Takako Nishi[2] · Yuko Matsuo[1]

Received: 13 June 2024 / Revised: 15 July 2024 / Accepted: 31 July 2024

Abstract

To sense light, animals often utilize mechanisms that rely on visual pigments composed of opsin and retinal. The photon-induced isomerization of 11-*cis*-retinal to the all-*trans* configuration triggers phototransduction cascades, resulting in a change in the membrane potential of the photoreceptor. In mollusks, the most abundant opsin in the eye is Gq-coupled rhodopsin (Gq-rhodopsin). The Gq-rhodopsin-based visual pigment is bistable, with the regeneration of 11-*cis*-retinal occurring in a light-dependent manner without leaving the opsin moiety. 11-*cis*-retinal is also regenerated by the action of retinochrome in the cell bodies. Retinal binding protein (RALBP) mediates retinal transport between Gq-rhodopsin and retinochrome in the cytoplasm. However, recent studies have identified additional bistable opsins in mollusks, including Opn5 and xenopsin. It is unknown whether these bistable opsins require RALBP and retinochrome for the continuous regeneration of 11-*cis*-retinal. In the present study, we examined the expression of RALBP and retinochrome in the photoreceptors expressing Opn5 or Xenopsin in the heterobranch gastropods *Limax* and *Peronia*. Our findings revealed that retinochrome, but not RALBP, was present in some of the Opn5A-positive brain photosensory neurons of *Limax*. The ciliary cells in the dorsal eye of *Peronia*, which express Xenopsin2, lacked both retinochrome and RALBP. Therefore, bistable opsins do not necessarily depend on the RALBP-retinochrome system in a cell. We also examined the expression of other proteins that support visual function, such as β-arrestin, Gq, and Go, in all types of photoreceptors in these animals, and uncovered differences in the molecular composition among the photoreceptors.

Keywords Onchidium · Extraocular photoreceptors · Retinoid cycle · Bistability · Cornea · α-tocopherol transfer protein

Introduction

Many animal photoreceptors rely on opsin-based photopigments to detect the ambient light. The chromophore retinal is covalently bound to the opsin protein by a Schiff base linkage in the 11-*cis* conformation in the dark state and isomerizes to all-*trans* upon photon absorption. Photoisomerization activates the phototransduction cascades in the photoreceptor, resulting in a change in membrane potential. To sustain the photoresponse under bright light conditions, isomerized retinal must be continuously regenerated back to its original 11-*cis* conformation.

In most vertebrate visual pigments in retinal photoreceptors, all-*trans*-retinal dissociates from an opsin protein and is transported to the adjacent retinal pigment epithelial (RPE) cells, where it is regenerated back to 11-*cis*-retinal through several enzymatic steps called the retinoid cycle (Palczewski and Kiser 2020; Choi et al. 2021; von Lintig et al. 2021). In the retinoid cycle, all-*trans*-retinal, dissociated from opsin, is

RRID: anti-RALBP antibody, AB_3101836; anti-limTTP antibody, AB_3101837; anti-Pero-retinochrome antibody (C-terminal, AB_3101839; N-terminal, AB_3101840); anti-PeroTTP antibody, AB_3101838.

Handling Editor: Kentaro Arikawa.

✉ Ryota Matsuo
matsuor@fwu.ac.jp

[1] Department of Environmental Sciences, International College of Arts and Sciences, Laboratory of Neurobiology, Fukuoka Women's University, 1-1-1 Kasumigaoka, Higashi-Ku, Fukuoka 813-8529, Japan

[2] Institute of Natural Sciences, Senshu University, Kawasaki, Japan

Published online: 09 August 2024

transported to RPE cells in a reduced form (all-*trans*-retinol) as a complex with interphotoreceptor retinoid binding protein (IRBP). All-*trans*-retinol is then enzymatically attached to phosphatidylcholine by ester bonding. The esterified all-*trans*-retinol is simultaneously isomerized and hydrolyzed to 11-*cis*-retinol by the catalytic activity of RPE65 (Moiseyev et al. 2005), followed by oxidation by 11-*cis*-retinol dehydrogenase 5 (RDH5), resulting in the production of 11-*cis*-retinal. The synthesis of 11-*cis*-retinol by RPE65 is promoted by cellular retinaldehyde-binding protein (CRALBP, also called retinaldehyde binding protein 1 or RLBP1), which binds 11-*cis*-retinoids, thereby suppressing the product inhibition of RPE65 by 11-*cis*-retinol. The regenerated 11-*cis*-retinal is then transported back to the photoreceptors by IRBP.

The regeneration of 11-*cis*-retinal is also accomplished by another biochemical pathway in the RPE and Müller glial cells through the action of retinal G protein-coupled receptor (RGR) in vertebrates (Choi et al. 2021; Tworak et al. 2023). In these cells, all-*trans*-retinol transported from the photoreceptors is oxidized to all-trans-retinal, which then binds to RGR in the endoplasmic reticulum. RGR catalyzes isomerization of all-*trans*-retinal to 11-*cis*-retinal in a light-dependent manner. The generated 11-*cis*-retinal is also thought to be protected from reverse re-isomerization by the presence of CRALBP in the RGR-mediated pathway (Zhang et al. 2019).

Although some cephalopods are predicted to possess RPE65-like genes (Zhang et al. 2021), an RPE65-dependent regeneration system has not been demonstrated in gastropods. Instead, opsins themselves have a bistable nature and are capable of light-dependent isomerization of bound all-*trans*-retinal back to the 11-*cis* configuration (Koyanagi and Terakita 2014). Mollusks also have an additional regeneration pathway that involves retinochrome (Hara and Hara 1967). Retinochrome is evolutionarily related to vertebrate RGR and is not coupled to intracellular G protein signaling (Shen et al. 1994; Matsuo et al. 2023). In the rhabdomeric photoreceptor, all-*trans*-retinal released from the bistable opsin is transported to retinochrome located in the membranous structures in the inner segment and re-isomerized to 11-*cis*-retinal in a light-dependent manner, similar to that of RGR (Hara and Hara 1967, 1980; Ozaki et al. 1983; Robles et al. 1987). Retinal-binding protein (RALPB) serves as a shuttle to transport all-*trans*- and 11-*cis*-retinal between Gq-coupled rhodopsin (Gq-rhodopsin) in the photoreceptor outer segment and retinochrome in the inner segment (Ozaki et al. 1987; Terakita et al. 1989). RALBP is evolutionarily related to vertebrate CRALBP/RLBP1 at the amino acid sequence level (Vöcking et al. 2021). Notably, a recent study demonstrated the expression of RLBP1 mRNA, which is predicted to encode a protein more closely related to CRALBP/RLBP1, in the larval eye of the polyplacophoran mollusk *Leptochiton asellus* (Vöcking et al. 2021). However, the RLBP1 gene is thought to be absent in all other molluscan species, and the functional role of this protein in *Leptochiton* remains to be investigated.

Gq-rhodopsin is the most abundant visual pigment in the rhabdomeric photoreceptors of the molluscan eye (Hara and Hara 1967; Nobes et al. 1992; Matsuo et al. 2019; Nishiyama et al. 2019). It transduces light information through the Gq signaling cascade, although a recent study reported simultaneous coupling to Go in the terrestrial slug *Limax* (Fig. S1a, Matsuo et al. 2023). However, several studies have shown that the eye photoreceptors of mollusks also express opsins belonging to different classes, such as Opn5 and Xenopsin (Yoshida et al. 2015; Vöcking et al. 2017; Matsuo et al. 2019, 2023; Döring et al. 2020). These opsins are bistable, and do not couple to Gq but to Gi/o (Yamashita et al. 2010; Kojima et al. 2011; Matsuo et al. 2023). Because Opn5s (Opn5A, Opn5B) and Xenopsin are co-expressed in the retinal photoreceptors of *Limax*, which also express Gq-rhodopsin (Matsuo et al. 2019, 2023), it is difficult to determine whether the visual pigments composed of Opn5s or Xenopsin require the aid of retinochrome for the recycling of retinal in the tentacular eye of *Limax*.

However, when focusing on the brain of *Limax*, some neurons express only Opn5A. In the cerebral ganglia, there is an Opn5A-positive neuronal cluster in the dorsal aspect (Matsuo et al. 2020, 2024), which is thought to contribute, at least in part, to the negative phototaxis behavior of slugs (Nishiyama et al. 2019). Therefore, these neurons are ideal research targets to test the requirement of a retinochrome-based regenerative system for Opn5-type bistable visual pigments.

There is another good subject to address this issue. The marine gastropod *Peronia verruculata* (formerly called *Onchidium verruculatum*) lives in the intertidal zone of rocky coasts and is equipped with a lot of extracephalic photoreceptors, called dorsal eye (DE) and dermal photoreceptor (DP), in the surface of its back, in addition to the cephalic eye, i.e. the stalk eye (SE), on the tip of their stalk (Bodington 1890; Weir 1899; Crozier and Arey 1919; Katagiri 1984, see Fig. S1b, c). We have recently demonstrated that the ciliary photoreceptors in the DE express only Xenopsin2 (Matsuo et al. 2022). Therefore, these cells are ideal targets for investigating the retinal recycling system of Xenopsin-based visual pigments.

In the present study, the expression of visual function-related genes was investigated in *Limax valentianus* and *Peronia verruculata*, focising on the retinoid cycle. We analyzed the expression of RALBP and retinochrome in the Opn5A-positive brain photosensory neurons of *Limax*, and in the SE, DE, and DP of *Peronia*. We also examined the expression of the alpha subunits of Gq and Go as well as β-arrestin, which attenuates opsin signaling by binding to the intracellular domain of opsin in many invertebrates,

including gastropods (Alvarez 2008; Gomez et al. 2011; Matsuo et al. 2017).

Materials and methods

Animals

The terrestrial slugs *Limax valentianus* (Férussac 1822, the synonym of *Ambigolimax valentianus*) were maintained in our laboratory as a closed colony for at least 42 generations. They were maintained in an incubator set at 19 °C, and fed a diet of humidified power consisting of 500 g of potato starch, 520 g of rat chow (Oriental Yeast, Tokyo, Japan), and 21 g of vitamin mixture (AIN-76, Oriental Yeast). Adult slugs (3–4 weeks post hatchling) were used in all the experiments. Adults of the marine systellommatophoran gastropod *Peronia verruculata* (Cuvier 1830, formerly called *Onchidium verruculatum*) were caught in the intertidal zone of Sakurajima, Kagoshima, Japan (31°34′47.7″ N, 130°35′49.3″ E). The body weight ranged from 10 to 30 g. They were kept in seawater at 14 °C for up to 3 weeks without feeding. The sea water was changed daily. For both animals, the light–dark cycle in the incubator was not strictly controlled, and the animals were under the influence of natural sunlight. However, the incubators were placed where they were not exposed to sunlight directly.

Molecular phylogenetic analyses

The amino acid sequences of RALBP and α-tocopherol transfer protein (α-TTP) from *Limax* and *Peronia* (abbreviated limRALBP, PeroRALBP, limTTP, PeroTTP, respectively) were aligned with SEC-14 CRAL-TRIO domain-containing proteins from a broad range of animals using MUSCLE (Edgar 2004). The alignment was visually inspected, and the ambiguously aligned sites were excluded prior to phylogenetic analyses using trimAl ver. 1.2 (Capella-Gutiérrez et al. 2009). The final dataset included 46 taxa with 360 sites. The alignment dataset is available from the corresponding author (R.M.) upon request. For the dataset, a maximum-likelihood (ML) analysis was carried out using IQ-TREE software (Nguyen et al. 2015), where the best amino acid substitution model was analyzed based on the minimum Bayesian information criterion value. The reliability of the phylogenetic tree was estimated with ultrafast bootstrap support (Minh et al. 2013) for 1,000 replicates. For this dataset, a Bayesian analysis was also conducted using MrBayes ver. 3.2 (Ronquist and Huelsenbeck 2003) with the LG + Γ model selected in IQ-TREE. Two independent runs of one cold and three heated Markov chain Monte Carlo (MCMC) with default chain temperatures were carried out for 1,000,000 generations, sampling trees at 100 generation intervals. The likelihood plot for both datasets suggested that the MCMC reached stationary phase after the first 25% of the trees (i.e. the first 250,000 generations were discarded as "burn-in"). Clade probabilities and branch length estimates were obtained from the remaining trees. GenBank accession numbers (acc. nos.) of the sequence data are shown in Table S1.

Reverse transcription-PCR (RT-PCR)

The brain, superior tentacle (ST), and ovotestis were dissected out from *Limax valentianus* under deep anesthesia with an injection (i.p.) of ice-cold Mg^{2+} buffer (57.6 mM $MgCl_2$, 5.0 mM glucose, and 5.0 mM HEPES, pH 7.0). The brain, tip of the tentacle including the stalk eye (SE), protrusions of the dorsal dermis (including the DE and DP), and ovotestis were dissected out from *Peronia verruculata* under deep anesthesia with ice-cold 0.5 M $MgCl_2$ injection (i.p.). Separation of DE and DP was not technically feasible because they were close to each other in the dermal protrusion (Fig. S1c). Total RNA was extracted from the tissues using an acid guanidinium thiocyanate-phenol–chloroform method (Chomczynski and Sacchi 1987), and the contaminating genomic DNA was degraded with DNase I. cDNAs were prepared by reverse transcription of the RNA using oligo-dT primer. The nucleotide sequences of PCR primers were 5'-GCCTGTAGATCTTGCTGGCTAC-3' and 5'-CGTAGCGATCCAGACTTCCGTC-3' for limRALBP (acc. no. LC820550), 5'-CTAAAGCAATCGCCTCCTTG-3' and 5'-ATAGACGAGGACTTGACGTG-3' for 18S rRNA of *Limax*, 5'-GATAAAGATGGGTCACCTGTCCG-3' and 5'-GCGCATCGAGGATTTCCATCG-3' for PeroRALBP (acc. no. LC820556), 5'-GTTAACCTGAGCCCATTTCTCC-3' and 5'-GGCAAGGCGGCAAAGTGAAC-3' for Pero-retinochrome (acc. no. BDL46495), 5'-CACAGTTCAGCATCCGCAGACTC-3' and 5'-CTGAACCTGTCTGCACCGATAACTC-3' for Pero-β-arrestin (acc. no. LC820555), 5'-GAGGTTCCTTAGATGACACGATCC-3' and 5'-TACGGGGCCTCGAAAGAGTC-3' for 18S rRNA of *Peronia*. The PCR products were electrophoresed in 1% agarose gel. The DNA bands were visualized using ethidium bromide under a UV illuminator.

Quantitative RT-PCR (qRT-PCR)

Quantification of cDNAs in each tissue sample was performed by the absolute quantification method using TB Green Premix Ex TaqII (Takara, Ohtsu, Japan) and Light Cycler96 System (Roche Diagnostics, Indianapolis, IN). cDNA samples were prepared from total RNA, as described above. The plasmids harboring the amplified cDNA regions were prepared and used as templates to delineate the calibration curves. Either pCRII (Thermo Fisher Scientific,

Waltham, MA) or pTA2 (TOYOBO, Osaka, Japan) was used as cloning vectors for the calibration plasmids. The nucleotide sequences of PCR primers were 5'-GTCTTCGACAAC ACCTTCAG-3' and 5'-TCGGCTCTCCGTGTCTGAG-3' for limRALBP, 5'-CTAAAGCAATCGCCTCCTTG-3' and 5'-ATAGACGAGGACTTGACGTG-3' for 18S rRNA of *Limax*, 5'-CTGATTTCTCCACCACCTTGC-3' and 5'-CGC ATCGAGGATTTCCATCG -3' for PeroRALBP, 5'-TGC ATAGTCGGTGTATCTACC-3' and 5'-GAGCCACGGCTT GCTACTG-3' for Pero-retinochrome, 5'-GGAGAAGCC TTTTACGGAGA-3' and 5'-TGAACTGTGGGACAGCAC TC-3' for Pero-β-arrestin, 5'-TGAGAAACGGCTACCACA TC-3' and 5'-CTCGAAAGAGTCCCGTATTG-3' for 18S rRNA of *Peronia*. The difference in the amount of template cDNAs was normalized according to the copy numbers of the cDNA of 18S rRNA. The experiment was performed with 4 biological replicates.

Toluidine blue staining

SE and DE (including the DPs) were isolated from anesthetized *Peronia* as described above and fixed in 4% paraformaldehyde dissolved in PBS for 1 h. Following washing in PBS for 1 h, the tissues were frozen in Tissue-Tek O.C.T. compound (Sakura Finetek, Tokyo, Japan) using liquid nitrogen. Frozen tissues were sectioned (14 µm-thick) in a cryostat and mounted onto CREST adhesive glass slides (Matsunami, Osaka, Japan). Sections were treated with neutralized formalin (Nakalai-Tesque, Kyoto, Japan) diluted to 5% in PBS for 20 min followed by a brief wash in PBS. The sections were stained with 0.02% toluidine blue for 4 min followed by several washes with water. The sections were further washed in 70% ethanol for 20 min to facilitate the removal of excess toluidine blue. The sections were coverslipped using PARA mount (Falma, Tokyo, Japan). Images were acquired using an Eclipse 600 microscope (Nikon, Tokyo, Japan) equipped with a DP70 CCD digital camera (Olympus, Tokyo, Japan) and a × 20 (NA 0.50) lens (Nikon).

Generation of antisera

Eight rabbit polyclonal antibodies were used for seven proteins in immunohistochemical experiments in this study: two different anti-Pero-retinochrome antibodies, anti-RALBP, anti-limTTP, anti-PeroTTP, anti-β-arrestin, anti-$G\alpha_q$, and anti-$G\alpha_o$ antibodies. One of the anti-Pero-retinochrome antibodies was raised against the C-terminal 14 amino acids (SFKSVLTGPEKKQE) that was conjugated to Keyhole limpet hemocyanin (KLH) by a Cys residue attached to the N-terminus of the peptide. The other anti-retinochrome antibody was raised against the N-terminal 20 amino acids (MTDETSMLSEEGLTNVAFNK) that was conjugated to KLH by a Cys residue attached to the C-terminus of the peptide. The anti-RALBP antibody was raised against 241–250 amino acids (GGKKTDPDGN) of limRALBP that was conjugated to KLH by a Cys residue attached to the N-terminus of the peptide. This peptide sequence was identical to the corresponding region in PeroRALBP (Fig. S2). Anti-α-TTP antibodies were raised against the C-terminal 19 amino acids of limTTP (acc no. LC820551, RGGVATD-SLVGTFKKLQTD) and of ProTTP (acc no. LC820552, EGGVATESLVGTFKKLSTE) conjugated to KHL by a Cys residue attached to the N-terminus of the peptide (Fig. S2). The peptide antibodies were affinity purified using the antigen peptides covalently attached to N-hydroxysuccinimide (NHS)-activated Sepharose 4 Fast Flow (GE Healthcare, Chicago, IL). Anti-β-arrestin antibody was previously raised against the full-length recombinant β-arrestin of *Limax valentianus* (Matsuo et al. 2017). Anti-$G\alpha_q$ and anti-$G\alpha_o$ antibodies were commercially obtained. According to the manufacturer, anti-$G\alpha_q$ antibody (anti-$G\alpha_{11}$ antibody, ZRB1446, Sigma-Aldrich, St. Louis, MO) was raised against the C-terminal 10 amino acids of human $G\alpha_{11}$, which are 100% identical to those of *Peronia* $G\alpha_q$ (acc. no. LC820553). Anti-$G\alpha_o$ antibody (#551, MBL, Tokyo, Japan) was raised against bovine $G\alpha_o$, which is 83% identical at the full length amino acid level to *Peronia* $G\alpha_o$ (acc. no. LC820554).

Cell culture and transfection of expression vectors

HEK293 cells were cultured on plastic or poly-L-lysine-coated glass-bottomed dishes (35 mm diameter, Matsunami, Osaka, Japan) in Dulbecco's modified Eagle medium (Fujifilm-Wako, Osaka, Japan) supplemented with 10% bovine serum at 37 °C in 5% CO_2-95% air. The cells were transfected with expression vectors using Lipofectamine3000 (Thermo Fisher Scientific) according to the manufacturer's instructions. The expression vectors were pcDNA4-hismax (Thermo Fisher Scientific) harboring the open reading frames of limRALBP, PeroRALBP, Pero-retinochrome, Pero-β-arrestin, $G\alpha_q$, $G\alpha_o$, limTTP, or PeroTTP. The cells were used for western blotting or immunocytochemistry 24 h after transfection.

Western blotting

The cells on the plastic dishes were lysed in ice-cold TNE (10 mM Tris (pH 7.4), 150 mM NaCl, 1 mM EDTA, 1% Nonidet P-40) supplemented with protease inhibitor cocktail (Fujifilm-Wako) and briefly sonicated to fragment genomic DNA. The isolated tissues were homogenized in TNE supplemented with protease inhibitor cocktail. Protein concentrations were determined using the PIERCE BCA protein assay kit according to the manufacturer's instructions (Thermo Fisher Scientific). The lysates were mixed with equal volumes of 2 × SDS sample buffer (4% SDS, 10%

glycerol, 10% β-mercaptoethanol, 50 mM Tris (pH 6.8), 0.1% bromophenol blue) and boiled at 100 °C for 4 min. The boiled samples (5 or 10 µg protein) were electrophoresed on SDS–polyacrylamide gels (SuperSep Ace 10–20% gradient gel, Fujifilm-Wako). Electrical transfer to nitrocellulose membrane (GE Healthcare), blocking and antibody reactions were performed as previously described (Matsuo et al. 2001). The concentrations of primary antibodies for RALBP (both *Limax* and *Peronia*), Pero-β-arrestin, limTTP, and PeroTTP were 0.1, 0.3, 0.1, and 0.1 µg/ml, respectively. The primary antibodies for $G\alpha_q$ (anti-$G\alpha_{11}$ antibody, ZRB1446, see above) and $G\alpha_o$ (#551, see above) were both used at 1:2000. As a loading control, mouse monoclonal anti-α-tubulin antibody (T5168, Sigma-Aldrich) was used at 1:5000. Anti-rabbit IgG or anti-mouse IgG antibodies conjugated with horse radish peroxidase (HRP, 1:10,000, GE Healthcare) were used as secondary antibodies. The luminescence signal was detected using Immunostar LD (Fujifilm-Wako) and LuminoGraph-I (Atto, Tokyo, Japan).

Immunocytochemistry

The HEK293 cells transfected with the expression vectors were washed in ice-cold PBS and fixed in 4% paraformaldehyde dissolved in PBS for 30 min. The cells were then permeabilized with 0.1% TritonX-100 dissolved in PBS (PBST) for 10 min. Following a brief wash in PBS, the cells were blocked in blocking buffer (2.5% goat serum, 2.5% bovine serum albumin dissolved in PBST) for 1–4 h. The cells were incubated with primary antibodies diluted in blocking buffer at 4 °C overnight. Mouse monoclonal anti-6 × His antibody (Proteintech, Rosemont, IL) was supplemented to the primary anti-RALBP, anti-Pero-retinochrome (C-terminus), anti-β-arrestin, anti-$G\alpha_q$, anti-$G\alpha_o$, anti-limTTP, or anti-PeroTTP antibody. The concentrations (or the dilution rates) of anti-6 × His, anti-RABP, anti-retinochrome (C-terminus), anti-β-arrestin, anti-$G\alpha_q$, anti-$G\alpha_o$, anti-limTTP, and anti-PeroTTP primary antibodies were 1:200, 0.1 µg/ml, 0.2 µg/ml, 0.3 µg/ml, 1:200, 1:500, 0.1 µg/ml and 0.1 µg/ml, respectively. Following three washes in PBS, the cells were incubated with Alexa488-labeled anti-rabbit IgG (1:500, Thermo Fisher Scientific) and Alexa594-labeled anti-mouse IgG (1:500, Thermo Fisher Scientific) diluted in blocking buffer for 1 h at room temperature. After washing in PBS, the cells were incubated with 0.1 µg/ml DAPI in PBS for 15 min, and washed again in PBS. Fluorescence images were acquired using a confocal laser scanning microscope C2 (Nikon) equipped with a × 40 objective lens (NA 0.95).

Immunohistochemistry

Tissues were isolated from deeply anesthetized *Limax* and *Peronia* as described above. In some experiments, neurobiotin (2% w/v) was incorporated from the cut end of the left optic nerve of the isolated brain of *Limax* at 14 °C overnight as previously described (Matsuo et al. 2014). The tissues were fixed in 4% paraformaldehyde dissolved in PBS for 1 h. After washing in PBS for 1 h, the tissues were rapidly frozen in Tissue-Tek O.C.T. compound using liquid nitrogen. Frozen tissues were sectioned (14 µm-thick) in a cryostat and mounted onto CREST adhesive glass slides. Following treatment with neutralized formalin solution diluted in half (final 5%) with PBS for 20 min, the sections were permeabilized with PBST for 10 min. After a brief wash in PBS, the sections were blocked in blocking buffer for 1–5 h at room temperature. The sections were then incubated with primary antibodies diluted in blocking buffer at 4 °C overnight. The concentrations (or the dilution rates) of anti-RABP, anti-Pero-retinochrome (C-terminus), anti-Pero-retinochrome (N-terminus), anti-β-arrestin, anti-$G\alpha_q$, anti-$G\alpha_o$ limTTP, and anti-PeroTTP primary antibodies were 0.1 µg/ml, 0.2 µg/ml, 0.6 µg/ml, 0.3 µg/ml, 1:200, 1:500, 0.1 µg/ml and 0.1 µg/ml, respectively. Anti-Opn5A and anti-Limax-retinochrome antibodies were used at 1.0 µg/ml and 0.2 µg/ml, respectively (Matsuo et al. 2019). For the pre-adsorption experiments of anti-RALBP, anti-$G\alpha_o$, anti-limTTP, and anti-PeroTTP antibodies, the antibodies were incubated in advance at 4 °C overnight with 0.1 µg/µl PeroRALBP, Pero-$G\alpha_o$, limTTP, and PeroTTP fused to the C-terminus of maltose-binding protein (MBP), respectively, which were bacterially expressed from the pMAL-c2 vector (NEB, Ipswich, MA) and purified using amylose resin (NEB) according to the manufacturer's instructions. Following three washes in PBS, the sections were incubated with secondary antibody (Alexa488-labeled anti-rabbit IgG) diluted in blocking buffer (1:500) for 1 h at room temperature. In some experiments, Alexa594-labeled streptavidin (1:1000, Thermo Fisher Scientific) was supplemented to the secondary antibody. Following a wash in PBS, the sections were incubated with 0.1 µg/ml DAPI in PBS for 15 min, and washed again in PBS. The sections were coverslipped with Fluoromount-G (SouthernBiotech, Birmingham, AL). Fluorescence images were acquired using an Eclipse 600 microscope equipped with a DP70 CCD digital camera and a × 10 (NA 0.45) or × 20 (NA 0.50) lens. For some experiments, fluorescence images were acquired using a confocal laser scanning microscope C2 equipped with a × 40 objective lens (NA 0.95).

Fluorescence in situ hybridization

The cDNAs corresponding to 1041–1610 bp of limRALBP and 482–904 bp of limTTP were ligated into the cloning vector pTA2. The plasmids were digested with appropriate restriction enzymes, and transcribed in vitro with T3 or T7 RNA polymerase (Roche Diagnostics, Seattle, WA). For

limRALBP, the cRNA probes were labeled with digoxigenin (DIG)-UTP (Roche Diagnostics). For limTTP, the cRNA probes were generated in the absence of labeling reagents, and were then labeled with 2,4-dinitrophenol (DNP) using the Label IT DNA labeling kit according to the manufacturer's instructions (Takara). For both genes, the final concentrations of the probes were adjusted so that the labeling titer was equivalent between antisense and sense probes. Hybridization and wash were performed as previously described (Fukunaga et al. 2006), except that the hybridization/wash temperature was 52 °C instead of 55 °C. DIG was detected using HRP-labeled anti-DIG antibody (1:800, Roche) and TSA plus fluorescein (AKOYA Biosciences, Marlborough, MA), while DNP was detected using alkaline phosphatase-labeled anti-DNP antibody (1:500, Vector Laboratories Newark, CA) and Fast Red TR Naphthol AS-MX tablets (Sigma-Aldrich, St. Louis, MO) as previously described (Matsuo and Matsuo 2022). For in situ hybridization of limRALBP only, the detection process of DNP-labeled cRNA probe was omitted from the procedure described above. The nuclei in the sections were labeled with 0.1 µg/ml DAPI before the coverslip with Fluoromount-G. Fluorescence images were acquired using an Eclipse 600 microscope equipped with a DP70 CCD digital camera and a×20 (NA 0.50) objective lens. Images of fluorescence signals with antisense and sense probes were acquired in the same exposure time.

Results

Identification of putative visual function-related genes

To identify visual function-related genes, other than retinochrome, β-arrestin, $G\alpha_q$, and $G\alpha_o$, expressed in *Limax* and *Peronia*, we searched for RALBP and RLBP1 in the transcriptome data (Matsuo et al. 2018, 2022) using RALBP and RLBP1 of *Leptochiton* as query sequences (Vöcking et al. 2021). For RALBP, we identified the sequence data of the cDNAs that were predicted to encode the homologues of RALBP in *Limax* and *Peronia*. These are 394 and 398 amino acids (Fig. S2), and the amino acid identities between RALBP of *Leptochiton* were 58% and 60%, respectively. The amino acid identity between RALBP of *Limax* and *Peronia* was 72% (Fig. S2). In the phylogeny reconstructed in this study, both were within the radiation of RALBP with 100% ML bootstrap probability (BP) and 1.00 posterior probability (PP), as expected (Fig. 1).

Although Vöcking et al. (2021) reported the absence of RLBP1 in gastropods, we tried to find its homologue from the transcriptome data of *Limax* and *Peronia*. The transcripts were identified from both databases with only moderate similarity to RLBP1 of *Leptochiton* (27% and 24% identical, respectively). Blast searches (blastp, https://blast.ncbi.nlm.nih.gov/Blast.cgi) against these proteins revealed higher similarities to α-tocopherol transfer protein (α-TTP) from several animals than to RLBP1. α-TTP is a member of the SEC-14 CRAL-TRIO domain-containing protein family, which also includes RALBP, RLBP1, and Clavesin (Panagabko et al. 2003; Saito et al. 2007; Smith and Briscoe 2015), and binds to vitamin E to facilitate its secretion from hepatocytes in mammals (Manor and Morley 2007; Kono and Arai 2015). In the molecular phylogenetic tree, the identified proteins of *Limax* and *Peronia* were within the radiation of α-TTP with 96% ML BP and 1.00 PP but not within that of RLBP1 (Fig. 1). The amino acid identity between α-TTP of *Limax* and *Peronia* was 73% (Fig. S2). Thus, we judged that these are the members of α-TTP group rather than RLBP1 group and named these genes limTTP and PeroTTP. Of note, however, we identified a recently registered data assigned to the clade of RLBP1 in the gastropod abalone, *Haliotis rubra* (GenBank acc. no. XP_046550909, Fig. 1).

In the following, we investigated the expression profiles of RALBP, retinochrome, and β-arrestin in the brain photosensory neurons of *Limax* and those of RALBP, retinochrome, β-arrestin, $G\alpha_q$, and $G\alpha_o$ in the visual systems of *Peronia.*

Expression of mRNAs for visual function-related genes

To investigate the expression of visual function-related genes, RT-PCR was performed using the RNA derived from different tissues of *Limax* and *Peronia*. For *Limax*, the brain, ST, and ovotestis were used. For *Peronia*, the brain, SE, DE/DP, and ovotestis were used. Electrophoresis of the PCR products revealed that in *Limax*, RALBP is expressed most abundantly in the ST (Fig. 2a). In *Peronia*, the expression of RALBP was low in the brain, whereas retinochrome showed higher expression in the brain and SE. β-Arrestin was ubiquitously expressed in all the tissues, but at a lower level in the ovotestis (Fig. 2c).

For a more quantitative analysis of expression levels, absolute qRT-PCR was performed. Relative expression levels among tissues were largely consistent with the electrophoresis images. In *Limax*, RALBP mRNA was expressed in the highest levels in the ST (Fig. 2b). In *Peronia*, RALBP mRNA was abundantly expressed in the SE (Fig. 2d), whereas retinochrome showed high copy numbers in the brain and SE (Fig. 2e). β-Arrestin showed a high level of expression in the brain and DE/DP, whereas it was expressed at a relatively low level in the ovotestis (Fig. 2f).

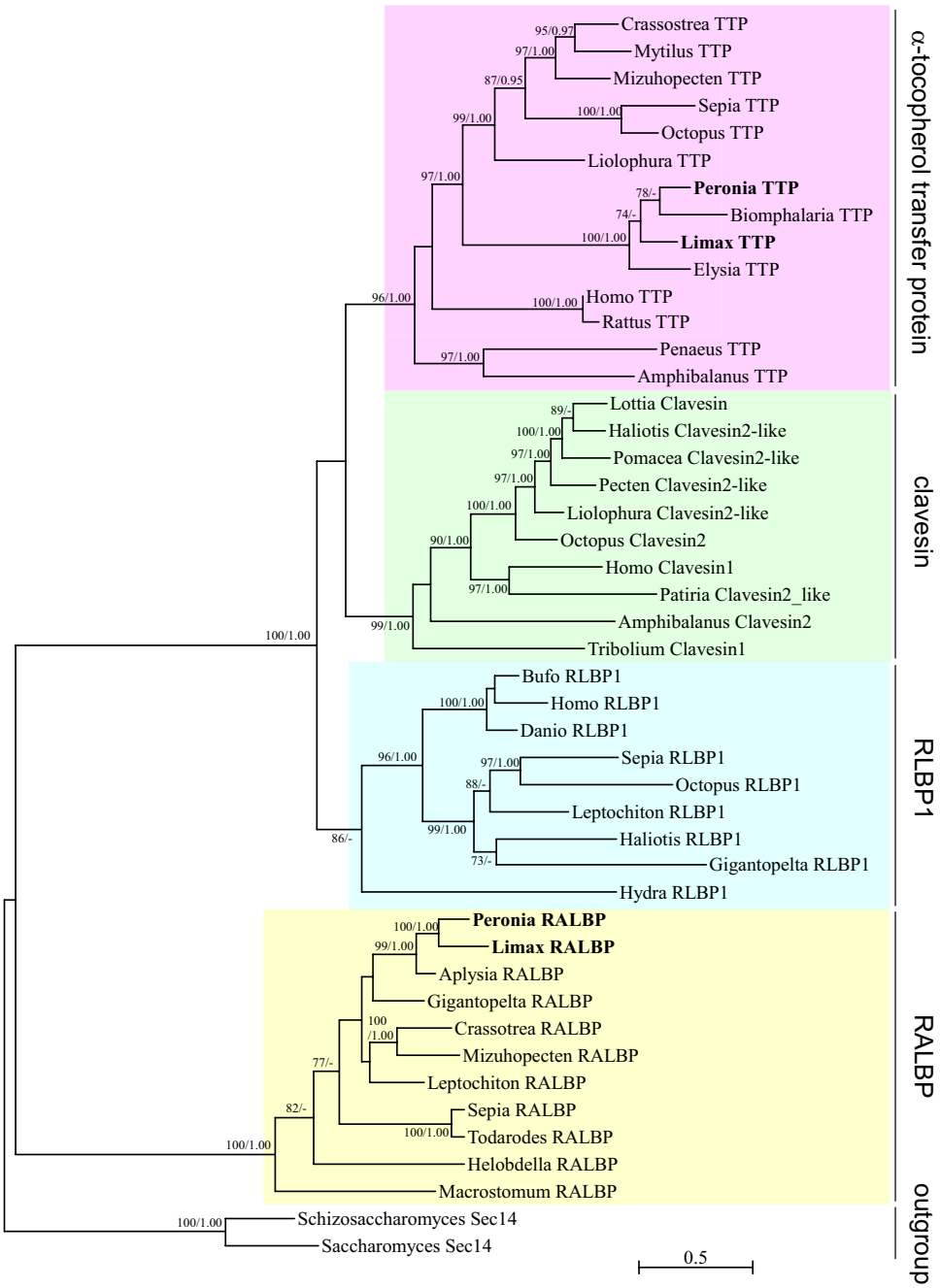

Fig. 1 A rooted molecular phylogenetic tree of the members of SEC-14 CRAL-TRIO domain-containing protein family. The tree was inferred from the amino acid sequences by the maximum likelihood (ML) method. The amino acid sequences of Sec14 of *Schizosaccharomyces pombe* and *Saccharomyces cerevisiae* serve as an outgroup. α-TTP and RALBP of *Limax* and *Peronia* are written in bold. Numerals at the branch nodes indicate the ML bootstrap probabilities (≥ 70%) and Bayesian posterior probabilities (≥ 0.95). The scale bar indicates 0.5 amino acid substitutions per site. See Table S1 for the GenBank accession numbers of the sequence data that appear in the tree

Generation and characterization of antibodies

To determine in which type of cells the visual function-related genes are expressed, we next examined the localization of the proteins by immunohistochemistry. To this end, antibodies were prepared for 5 different visual function-related proteins, RALBP, retinochrome, β-arrestin, $G\alpha_q$, and $G\alpha_o$. The antibody against α-TTP was also prepared. For retinochrome and α-TTP, the antibodies were generated each for *Limax* and *Peronia*, respectively. For RALBP, $G\alpha_q$, $G\alpha_o$, and β-arrestin, the same antibody was used for both *Limax* and *Peronia*. The antibody against RALBP was raised against the peptide whose sequence is identical between *Limax* and *Peronia* (Fig. S2). The antibodies against $G\alpha_q$ and $G\alpha_o$ were commercially available and were raised against human $G\alpha_{11}$ and bovine $G\alpha_o$, respectively (see Materials and Methods for detail). The antibody against β-arrestin was previously generated using the full-length recombinant protein of *Limax* β-arrestin (lim-β-arrestin) as an antigen (Matsuo et al. 2017) whose amino acid sequence is 86% identical to Pero-β-arrestin (data not shown). The antibodies against the C-terminal peptides of α-TTP of *Limax* and *Peronia* were

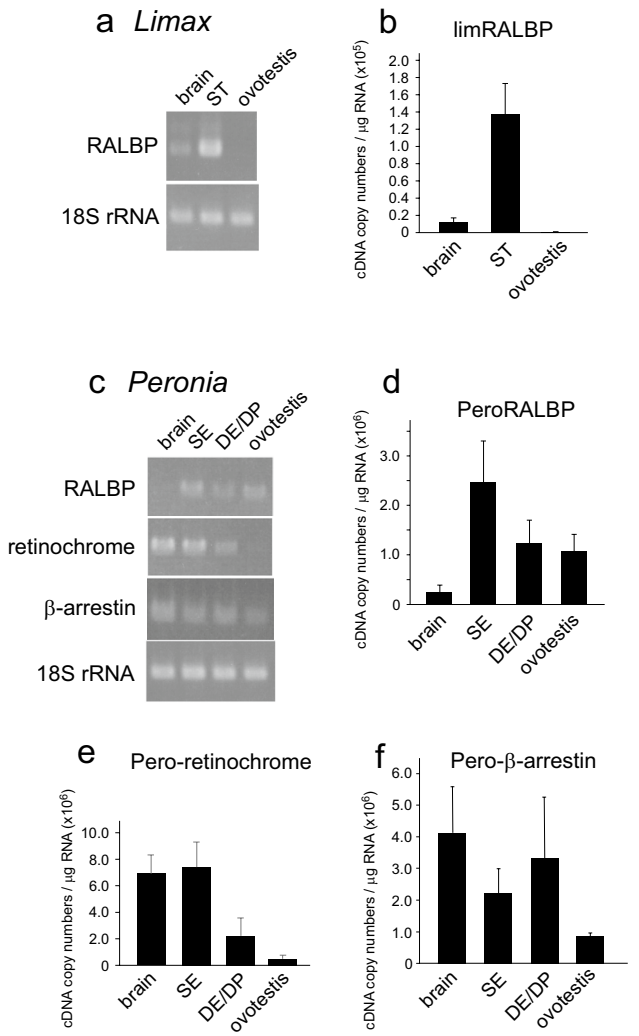

Fig. 2 Expression of visual function-related genes in different tissues. **a.** RT-PCR of limRALBP using the RNA derived from the brain, ST, and ovotestis of *Limax*. **b.** qRT-PCR of limRALBP. **c.** RT-PCR of PeroRALBP, Pero-retinochrome, and Pero-β-arrestin using the RNA derived from the brain, SE, DE/DP and ovotestis of *Peronia*. **d-f.** qRT-PCR of **d** Pero-RALBP, **e** Pero-retinochrome, and **f** Pero-β-arrestin. Error bars indicate SE (n = 4). The bands of 18S rRNA serve as an internal control for the equivalent cDNA amounts among tissues. ST, superior tentacle; SE, stalk eye; DE, dorsal eye; DP, dermal photoreceptor

also generated (Fig. S2). Since the antibody against the C-terminus of *Limax* retinochrome was previously generated and characterized (Matsuo et al. 2017), the antibodies against the C- and N-termini of Pero-retinochrome were raised in the present study. The specificities of the antibodies were confirmed as follows.

The specificity of the anti-RALBP antibody in the tissue of *Limax* and *Peronia* was examined immunocytochemically in HEK293 cells expressing 6 × His-tagged limRALBP and 6 × His-tagged PeroRALBP (Figs. S3a, S4a). Western blotting of their lysates revealed single bands with almost predicted molecular sizes, ca. 48 and 49 kDa for 6 × His-limRALBP and 6 × His-PeroRALBP, respectively (Figs. S3b-left, S4b). Western blotting of the tissue lysates of *Limax* also showed a single band of RALBP only in the lysate of ST with a slightly smaller molecular size due to the absence of 6 × His tag (Fig. S3b-right). This expression pattern of endogenous RALBP is in agreement with the result of qRT-PCR (Fig. 2a, b). Pre-adsorption with recombinant MBP-PeroRALBP protein diminished the immunoreactive signals in the DP of *Peronia*, further corroborating the applicability of this antibody to the tissue of *Peronia* (Fig. S4c). Taken together, the anti-RALBP antibody specifically recognized RALBP of both *Limax* and *Peronia*.

Anti-Pero-retinochrome antibody raised against the C-terminal 14 aa recognized N-terminally 6 × His-tagged Pero-retinochrome expressed in HEK293 cells, and the immunosignals overlapped with those of 6 × His (Fig. S5a). To further validate the specificity of the anti-retinochrome antibody, another antibody was raised against the N-terminal 20 amino acids of retinochrome of *Peronia*. The antibody against the N-terminus showed the same staining patterns in the SE and DP (Fig. S5b, c).

Characterization of anti-β-arrestin, anti-$G\alpha_q$, anti-$G\alpha_o$ and anti-α-TTP antibodies were also performed, and the detail is described in the Supplementary text and Figs. S6-S9.

Localization of visual function-related proteins in the visual system of *Limax*

We next examined the localization of visual function-related proteins in *Limax* photosensory cells by immunohistochemistry. Since the localization of retinochrome, β-arrestin, $G\alpha_q$, and $G\alpha_o$ has already been reported in the tentacular eye of *Limax* (Matsuo et al. 2017, 2023), we first examined the localization of RALBP in the eye and the brain.

Immunostaining of RALBP in the horizontal section of the tentacular eye of *Limax* revealed the signals in the cell body layer of the retina and in the optic nerves (Fig. 3a). The rhabdomeric region also exhibited immunosignals to a lesser extent (Fig. 3a, b). Interestingly, the cornea of the eye also exhibited the immunosignal of RALBP (Fig. 3a, b). Localization in the cornea is unexpected because other visual function-related proteins, such as retinochrome, opsins, $G\alpha_q$, $G\alpha_o$ or β-arrestin, have never shown immunosignals in the cornea (Matsuo et al. 2017, 2019, 2023). For example, retinochrome was localized primarily to the cell body layer of the retina with no signal in the cornea (Fig. 3b lower panels, Matsuo et al. 2017). It is unlikely that the signal in the cornea was due to non-specific binding of the antibody to the cornea, because the protein of α-TTP, whose mRNA was co-expressed with that of RALBP in the retina (Fig. S10a), was also localized to the cornea of the *Limax* eye (Fig. S10b). In addition, mRNA of RALBP was detected in the cornea by

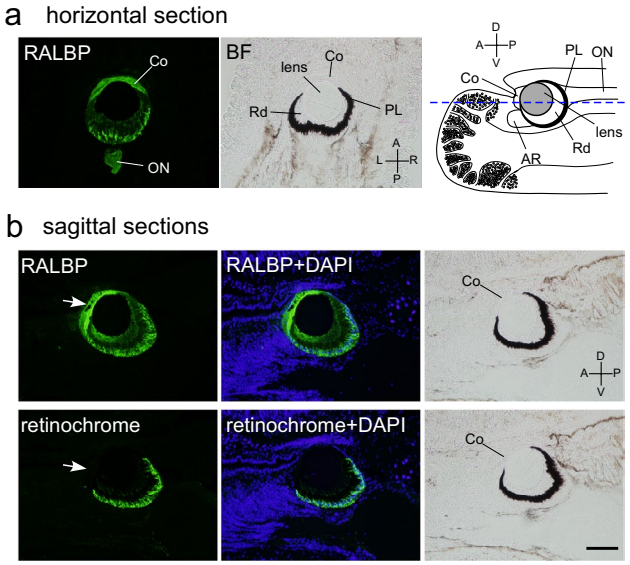

Fig. 3 Localization of RALBP in the eye of *Limax*. **a.** Immunosignals of RALBP in the horizontal section of an eye. A cartoon on the right explains the cutting plane in the superior tentacle. **b.** Immunosignals of RALBP and retinochrome in the neighboring sagittal sections of an eye. White arrows indicate the cornea. Scale bar: 100 µm. BF, bright field image; PL, pigment layer; Rd, rhabdomere; Co, cornea; ON, optic nerve; AR, accessory retina; A, anterior; P, posterior; R, right; L, left; V, ventral; D, dorsal

in situ hybridization in the section where the cell bodies of cornea appeared (Fig. S10c).

The presence of immunosignals in the rhabdomeric layer of the eye (Figs. 3, S10b) suggests that RALBP is expressed at least in Type-I photoreceptors, since this layer consists of the microvillous domain of Type-I photoreceptors (Brandenburger 1975; Kataoka 1975; Katagiri et al. 2001; Zieger and Mayer-Rochow 2008). However, there is no denying the possibility that the protein is also localized to Type-II photoreceptors, which are equipped with tiny, less developed microvilli, making it difficult to resolve the immunoreactive signals there. We have recently demonstrated that Type-I and Type-II photoreceptors project to distinct targets, the optic neuopile, in the *Limax* cerebral ganglion, where the former projects to the medial lobe of the optic neuropile and the latter to the lateral lobe (Matsuo et al. 2024, see also the cartoon in Fig. 4). We thus exploited this observation to determine in which type of photoreceptor RALBP is expressed. The optic neuropiles in the cerebral ganglia were visualized by neurobiotin (NB) incorporated from the cut end of the left optic nerve, and we determined which lobe was stained with anti-RALBP antibody. As shown in Fig. 4 (upper), the immunoreactivity of RALBP overlapped with the signal of NB. Anti-β-arrestin antibody, which stains optic nerves (Matsuo et al. 2017), also showed the immunosignals in both lobes (Fig. 4 lower). These results indicate that RALBP and β-arrestin are expressed in both Type-I and Type-II photoreceptors in the retina of *Limax*.

We next investigated whether Opn5A-positive brain photosensory neurons express visual function-related proteins. The Opn5A-positive neuronal cluster in the dorsal aspect of the cerebral ganglion can be visualized by NB incorporated from the cut end of the contralateral optic nerve because these Opn5A-positive brain neurons are connected to the optic neuropile in the contralateral hemiganglion

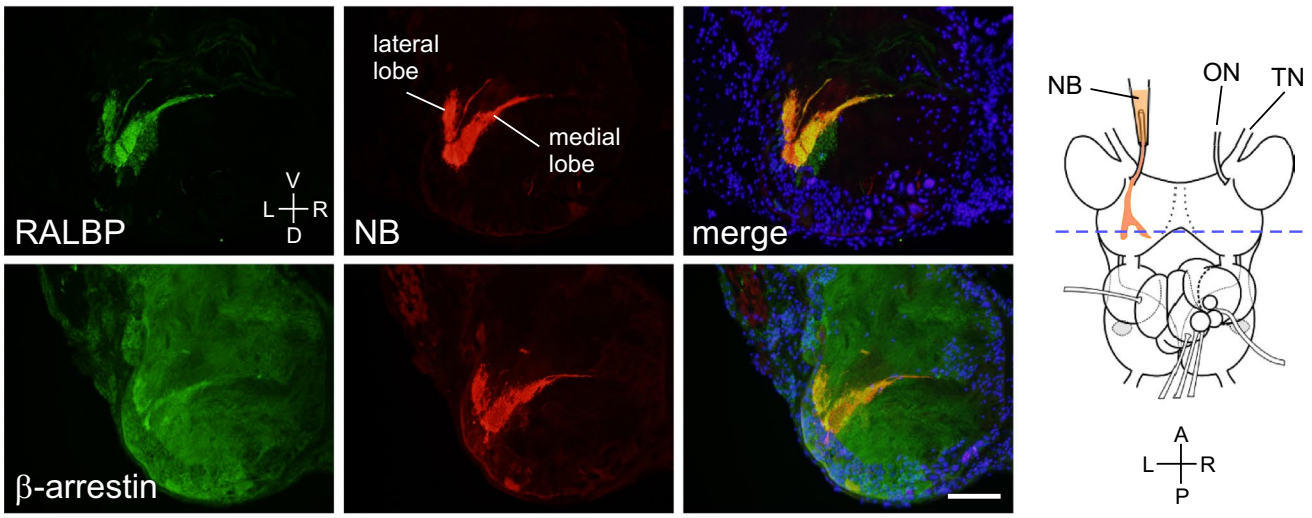

Fig. 4 Immunosignals of RALBP and β-arrestin in the optic neuropile in two neighboring coronal sections of the cerebral ganglia of *Limax*. The signals are visible in the both lobes of optic neuropile. Right panels are the images of immunoreactive signals of RALBP or β-arrestin superimposed over the signals of NB (red) and DAPI (blue). A cartoon on the right explains the cutting plane of the sections. Scale bar: 100 µm. NB, neurobiotin; A, anterior; P, posterior; R, right; L, left; V, ventral; D, dorsal

by gap junctions (Matsuo et al. 2020). Dual staining with specific antibodies against visual function-related proteins and fluorescent streptavidin revealed that RALBP was not localized to the Opn5A-positive cluster (white arrowheads in Fig. 5a). In contrast, the immunoreactivity of retinochrome overlapped with the signal of NB (arrows in Fig. 5b). The expression of retinochrome in the Opn5A cluster was also corroborated by the immunostaining of retinochrome and Opn5A alternately in the serial sections of the other part of the cerebral ganglia (white arrowheads in Fig. S11). However, depending on the location, some Opn5A-positive neurons did not co-express retinochrome (yellow arrows in Fig. S11d). For β-arrestin, it was expected that there would be overlaps to some extent because β-arrestin is ubiquitously expressed in all tissues (DeWire et al. 2007). But the overlapping was not conspicuous in the Opn5A-positive cluster (Fig. 5c).

Localization of visual function-related proteins in the visual system of *Peronia*

Next, the localization of visual function-related proteins was examined immunohistochemically in *Peronia*. In the SE, RALBP was localized primarily in the cell body layer, and the signal in the rhabdomere was weak (Fig. 6a). Like in the eye of *Limax*, there was also an immunosignal in the cornea (yellow arrowheads in Fig. 6). In the DE, no signal was found in either the lens cell or ciliary cells, whereas intense immunoreactive signals were found in the DP. There were also weak immunoreactive signals in small cells just beneath the surface of the dermis, although the identity of the cells is unclear (white arrowheads in Fig. 6a). Further examination by confocal microscopy revealed that RALBP was more abundant in the cell body region than in the microvillus region of the DP (Fig. 6b).

The localization of retinochrome and β-arrestin was also examined in *Peronia*. In the SE, the immunosignal of retinochrome was restricted to the cell body layer (Fig. 7a), as in the eye of *Limax* (Fig. 3b). No signal was found in the DE, whereas the DP exhibited strong immunoreactivity of retinochrome (Figs. 7a, S4c). In the SE, the immunosignal of β-arrestin was observed in the rhabdomere (Fig. 7b). The DP and ciliary cells in the DE also exhibited strong immunosignals, but the lens cell of the DE did not (Fig. 7b). Observation of the DPs by confocal microscopy revealed more clearly that retinochrome was widely distributed throughout the cell, whereas β-arrestin was restricted to the microvillus portion of the DP (right panels of Fig. 7a, b).

Finally, the localization of $G\alpha_q$ and $G\alpha_o$ was examined in *Peronia*. Immunosignals of $G\alpha_q$ and $G\alpha_o$ were detected in the rhabdomere of the SE and in the whole cell body of the DP (Fig. 8a, b). They appeared even in neighboring sections

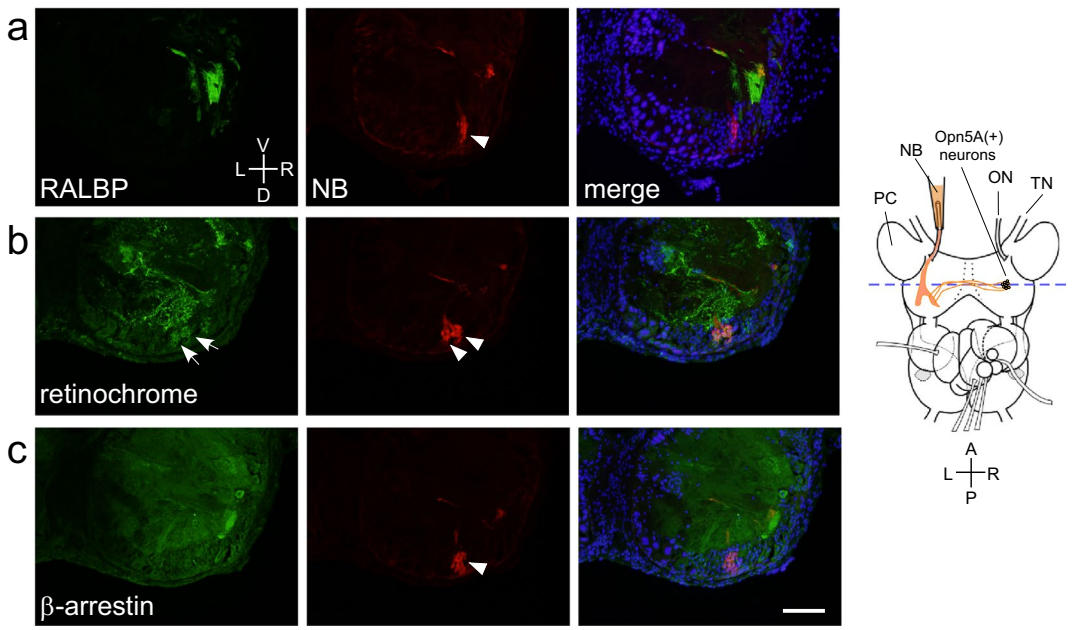

Fig. 5 NB-incorporating Opn5A cluster in the cerebral ganglion of *Limax* does not express RALBP but does retinochrome. White arrowheads in the middle panels indicate the Opn5A cluster incorporating NB delivered from the cut end of the contralateral optic nerve. Yellow arrowheads indicate the signals of NB in the terminal of commissure. **a.** Dual staining of RALBP and NB in the coronal section of the cerebral ganglia. **b.** Dual staining of retinochrome and NB in the coronal section of the cerebral ganglia. White arrows in the left panel indicate the immunosignals of retinochrome that overlap those of NB. **c.** Dual staining of β-arrestin and NB in the coronal section of the cerebral ganglia. A cartoon on the right explains the cutting plane of the sections. Scale bar: 100 μm. NB, neurobiotin; ON, optic nerve; PC, procerebrum; TN, tentacular nerve

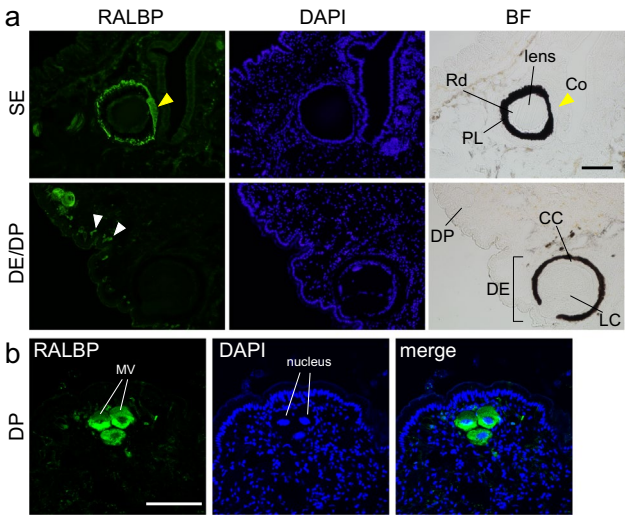

Fig. 6 Localization of RALBP in the photosensors of *Peronia*. **a.** Immunoreactivity of RALBP in the SE (upper), DE, and DP (lower). Micrographs of RALBP immunoreactivity were taken in the same exposure time between the SE and DE/DP. Yellow arrowheads indicate the cornea. White arrowheads indicate the immunoreactive small cells beneath the surface of the dermis. **b.** An image of RALBP in the DP acquired with a confocal laser scanning microscope. Co, cornea; DE, dorsal eye; LC, lens cell of DE; CC, ciliary cell of DE; DP, dermal photoreceptor; SE, stalk eye; PL, pigment layer; Rd, rhabdomere; MV, microvilli. Scale bars: 100 µm

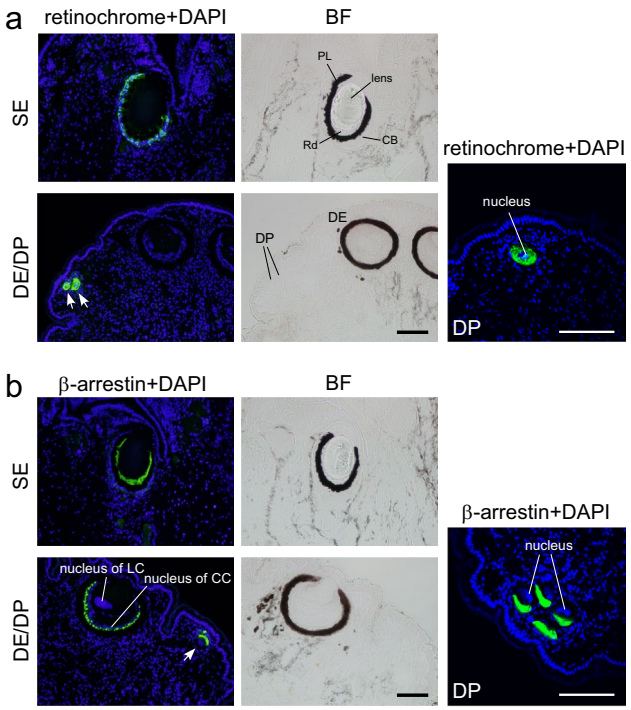

Fig. 7 Localization of retinochrome and β-arrestin in the photosensors of *Peronia*. **a.** Immunoreactivity of retinochrome using the antibody against C-terminus of Pero-retinochrome in the SE and DP. White arrows indicate DP. Images of SE and DE/DP were taken in the same exposure time. **b.** Immunoreactivity of β-arrestin in the SE, DE, and DP. White arrows indicate DP. Images of SE and DE/DP were taken in the same exposure time. Right panels are the superimposed images of retinochrome/β-arrestin immunoreactivity over the fluorescence of DAPI acquired with a confocal laser scanning microscope. BF, bright field image; SE, stalk eye; DP, dermal photoreceptor, DE, dorsal eye; Rd, rhabdomere; PL, pigment layer; CB, cell body layer; LC, lens cell; CC, ciliary cell. Scale bars: 100 µm

of the SE cut in 10 µm thick (Fig. S12). Since the diameter of the Type-I photoreceptor in the SE slightly exceeds 10 µm (Katagiri et al. 2001), both proteins were expected to be co-localized in a Type-I photoreceptor. Weak immunoreactive signals of $G\alpha_q$ were also detected in the lens cells and ciliary cells of the DE (Fig. 8a). Immunosignals of $G\alpha_o$ were detected in both the cell body layer and the rhabdomeric layer of the SE. The DP and the ciliary cells of the DE also exhibited immunosignals, but the lens cells of the DE did not (Fig. 8b).

Discussion

The results of the present study are summarized in Table 1. We demonstrated that Opn5A-expressing *Limax* brain photosensory neurons and Xenopsin2-expressing *Peronia* DE ciliary cells do not necessarily have all the known visual function-related proteins in the same cell. For example, the Opn5A-positive neuronal cluster in the cerebral ganglia does not express RALBP despite some of them contain retinochrome. The components of the DE of *Peronia*, i.e. the lens cells and ciliary cells, have neither retinochrome nor RALBP. The lens cells also lack prominent expression of β-arrestin, although it is uncertain at present even whether they contain opsin-based photopigments or not.

In contrast, the Type-I photoreceptors in the SE and the DP of *Peronia* are equipped with the same set of visual function-related proteins as far as we have investigated. Retinochrome and RALBP are known to function in the regeneration of 11-*cis*-retinal in Gq-rhodopsin-expressing-photoreceptors of mollusk (Hara and Hara 1967, 1980; Ozaki et al. 1983, 1987, 1994; Molina et al. 1992; Terakita et al. 1989). Because the Type-I photoreceptors in the SE and the DP of *Peronia* express the same set of opsin proteins, including Gq-rhodopsin and Xenopsin1 (Matsuo et al. 2022), it is reasonable that both photoreceptors have the same set of visual function-related proteins. The subcellular localizations of RALBP, retinochrome, and β-arrestin in the DP were also similar to those in Type-I photoreceptors (Figs. 3, 6, 7). Taking into account that both the Type-I photoreceptors in the SE and the DP have the identical spectral sensitivity (peak at 500 – 520 nm, Katagiri et al. 1985), the DPs can be

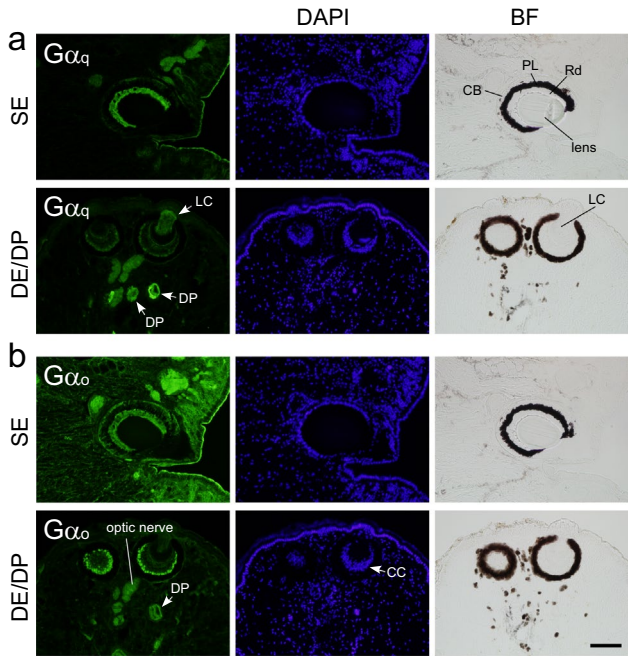

Fig. 8 Localization of $G\alpha_q$ and $G\alpha_o$ in the photosensors of *Peronia*. **a.** Immunosignals of $G\alpha_q$ in the SE, DE, and DP. **b.** Immunosignals of $G\alpha_o$ in the SE, DE, and DP. Images of SE and DE/DP were taken in the same exposure time. BF, bright field image; SE, stalk eye; DP, dermal photoreceptor, DE, dorsal eye; Rd, rhabdomere; PL, pigment layer; CB, cell body layer; LC, lens cell; CC, ciliary cell. Scale bar: 100 µm

considered as if they are the Type-I photoreceptors of the SE widely distributed in the surface of the dorsal dermis of *Peronia*.

The alpha subunits of Gq and Go of *Peronia* were both expressed in the Type-I photoreceptors in the SE. This is consistent with our previous observation in the tentacular eye of *Limax* (Matsuo et al. 2023). We have also reported in *Limax* that Gq couples with Gq-rhodopsin whereas the Go couples with all of Gq-rhodopsin, Xenopsin and Opn5A/B in vitro (Matsuo et al. 2023). Since Type-I photoreceptors in the SE of *Peronia* co-express Xenopsin1 and Gq-rhodopsin, Xenopsin1 would be the counterpart of Xenopsin of *Limax* with respect to localization as well as sequence similarity and phototransduction cascade. Therefore, the Type-I photoreceptors in the eyes of *Limax* and *Peronia* are very similar in terms of molecular composition and signal transduction, although the opsin corresponding to Opn5A/B of *Limax* has not been identified in the SE of *Peronia*.

In the ciliary cells of the DE of *Peronia*, $G\alpha_o$ exhibited a more prominent expression compared to $G\alpha_q$ (Fig. 8). Go is expected to couple with Xeopsin2 in the ciliary cells, like Xenopsin of *Limax* due to the similarity of amino acid sequence. If Xenopsin2 preferentially couples to Go in the ciliary cells, it would also do so in the Type-II photoreceptors in the retina of *Peronia*, because in the retina, Xenopsin2 is expressed in Type-II photoreceptors (Matsuo et al. 2022). Considering that Gi is absent from the *Limax* retina (Matsuo et al. 2023), our previous and present results strengthen the view that visual pigments composed of Xenopsin family proteins transduce intracellular photosignaling through Go in heterobranch gastropods. Further studies are needed to elucidate the role of Gq detected at a relatively low level in the ciliary cells of the DE.

Table 1 Summary of the expression of visual function-related proteins

	Limax				*Peronia*				
	Tentacular eye		Brain		Stalk eye		Dorsal eye		
	Type-I	Type-II	Opn5A cluster		Type-I	Type-II	Lens cell	Ciliary cell	Dermal photoreceptor
Gq-rhodopsin[*1]	++	−	−	Gq-rhodopsin1/2[*1]	++	ND	−	−	++
Xenopsin[*1]	++	ND	−	Xenopsin1[*1]	++	ND	−	−	++
Opn5A[*1]	++	ND	++	Xenopsin2[*1]	−	++	−	++	−
Opn5B[*1]	++	ND	−	Opn5B[*1]	ND	ND	ND	ND	ND
retinochrome	++[*2]	ND	+	retinochrome	++	ND	−	−	++
RALBP	++	++	−	RALBP	++	ND	−	−	++
β-arrestin	++	++	±	β-arrestin	++	ND	−	++	++
$G\alpha_q$	++[*3]	ND	ND	$G\alpha_q$	++	ND	+	±	++
$G\alpha_o$	++[*3]	ND	ND	$G\alpha_o$	++	ND	−	++	++

"++", "+", "±", and "-" indicate high, mediam, low, and no protein expression, respectively. ND, Not determined

[*1]Expression of opsins was determined in Matsuo et al. (2019, 2020, 2022, 2023)

[*2]Expression of retinochrome in Type-I photoreceptor was demonstrated in Matsuo et al. (2019)

[*3]Expression of $G\alpha_q$ and $G\alpha_o$ in Type-I photoreceptor was demonstrated in Matsuo et al. (2023)

In the lens cells of the DE, the microvillus region was moderately immunostained with anti-$G\alpha_q$ antibody (Fig. 8a). This observation implies the presence of some Gq-coupled rhodopsin in this cell. A previously uncharacterized Gq-rhodopsin-like opsin, which was identified only in the transcriptome data, may be expressed in the lens cell (Matsuo et al. 2022). However, the presence of Gq does not necessarily indicate the presence of Gq-coupled rhodopsin. Therefore, further careful investigation is needed in the future to determine the identity of the photosensory molecule in the lens cell.

The prominent expression of β-arrestin in the ciliary cells of the DE suggests that β-arrestin attenuates the activation of not only Gq-rhodopsin in the Type-I retinal photoreceptors but also of Xenopsin2 in the ciliary cells of the DE. Taking into account that β-arrestin is present in the both terminals of Type-I and Type-II photoreceptors in the *Limax* cerebral ganglia (Fig. 4), β-arrestin is expected to be functional in attenuating the photosignaling in both types of retinal photoreceptors in heterobranchia. This view is consistent with the fact that Xenopsin2 is expressed in the Type-II photoreceptors in *Peronia* (Matsuo et al. 2022). In contrast, there was no prominent expression of β-arrestin in the lens cell of the DE (Fig. 7b). It has not been clarified what type of photosensitive molecules are expressed in the lens cells despite they exhibit depolarizing photoresponse (Yanase et al. 1981; Katagiri et al. 1985). If the lens cell contains photosensitive molecules other than opsin-based visual pigments, they would be able to terminate the photoresponse without the aid of β-arrestin.

It is intriguing that the Opn5A-expressing neuronal cluster in the slug's brain expresses retinochrome but not RALBP (Fig. 5). This suggests that retinal transport is not mediated by RALBP. Direct exchange of retinal has been proposed to occur between Gq-rhodopsin and retinochrome in the basal region of the rhabdomeric photoreceptor of cephalopod eye because these two opsin proteins colocalize at the base of the rhabdomere (Hara and Hara 1973; Ozaki et al. 1983). In fact, direct chromophore exchange among rhodopsins and color opsins has been reported to occur in the eye of vertebrates (Matsumoto et al. 1975; Defoe and Bok 1983). Because Opn5A-expressing neurons are small and lack specialized rhabdomeric cellular compartments (Matsuo et al. 2020), direct interaction between Opn5A and retinochrome may be more likely to occur. However, we also found some Opn5A-expressing neurons that did not even contain retinochrome in the brain of *Limax* (Fig. S11). Future studies are awaited to elucidate how such Opn5A-expressing neurons recover 11-*cis*-retinal. As for G proteins, it was difficult to determine the identity of Gα expressed in Opn5A-expressing neuronal cluster because both $G\alpha_q$ and $G\alpha_q$ are ubiquitously expressed in the brain, especially in the neuropile region (Fig. S13).

Furthermore, we identified many retinochrome-expressing neurons in the brain of *Limax*, and their number far exceeded that of Opn5A-experssion neurons (Matsuo et al. 2020). In fact, many of the retinochrome-immunopositive cell bodies did not express Opn5A (e.g. see Fig, S14k1, 2). We also found that the cerebral giant cells located in the ventral aspect of the cerebral ganglia were strongly immunostained with anti-retinochrome antibody (yellow arrowheads in Fig. S14g-i). Cerebral giant cells are known to regulate the feeding rhythm in the pond snail *Lymnaea stagnalis* (McCrohan and Benjamin 1980; Yeoman et al. 1996), and the role of retinochrome in such cells is unclear.

Overall, it is difficult to explain the role of retinochrome expressed alone in the brain neurons. Retinoids, however, are known to function not only in opsin-based vision, but also in transcriptional regulation in the nervous system of vertebrates (Maden 2002). In *Lymnaea*, retinoids affect the electrical activity and synaptic plasticity of neurons, which do not necessarily seem photosensitive (Vesprini et al. 2015; de Hoog et al. 2019; Wingrove et al. 2023). In the central nervous system of *Ciona intestinalis*, studies conducted by Tsuda group demonstrated the expression of retinochrome/RGR-like gene in the neurons that lack the expression of opsins, and the role of retinochrome as a retinoid receptor was proposed (Nakashima et al. 2003; Tsuda et al. 2003). Although lipid-soluble retinoids are generally thought to enter cells without specific membrane transporters, their receptors on the outer and/or inner membrane structures would facilitate their incorporation and capture.

The immunostaining of RALBP in the retina of *Limax* does not provide information regarding the expression of this protein in either Type-I or in both Type-I and Type-II photoreceptors due to spatial limitation (Kataoka 1975). However, our findings indicate that both lobes of the optic neuropile were immunopositive for RALBP (Fig. 4). This observation suggests that both Type-I and Type-II photoreceptors express RALBP, as is the case with β-arrestin. Although the Type-I but not Type-II photoreceptors were shown to express Gq-rhodopsin in *Limax* (Matsuo et al. 2024), the repertoire of opsin species in Type-II photoreceptors remains to be unambiguously determined. Therefore, it is not clear to what opsin RALBP transports 11-*cis*-retinal in the Type-II photoreceptors of *Limax*.

We also found that the ciliary cells in the DE do not express retinochrome or RALBP. This observation is consistent with the previous report by Katagiri et al. (2002) that failed to detect the presence of retinochrome in the DE of *Peronia* using a fluorescence histochemical method. Our findings indicate that, unlike Gq-rhodopsin, Xenopsin2 does not require the RALBP-retinochrome system within the same cell for its chromophore regeneration. It is currently not possible to state with certainty that Xenopsin2 can regenerate all necessary 11-*cis*-retinal on its own by its

bistability. The presence of the aid from other surrounding cells, like the retinoid cycle in the RPE cells of mammalian retina, cannot be denied at present.

Intrinsically photosensitive retinal ganglion cells (ipRGC) of mammals possess melanopsin-based visual pigments, which exhibit a bistable nature. Although it was controversial whether melanopsin in ipRGC requires RPE65-dependent retinoid cycle for the recovery of 11-*cis*-retinal (Doyle et al. 2006; Tu et al. 2006), a recent study suggested that Müller glial cells mediate the transport of retinal between ipRGC and RPE cells using RLBP1 protein (Harrison et al. 2021). Therefore, bistable visual pigments do not always depend on a cell-autonomous regenerative system. The existence of such an intercellular transport system for retinal regeneration remains unconfirmed in the molluscan visual system, and further investigation is awaited.

The expression pattern of αTTP coincided with that of RALBP as far as we investigated (Figs. S4, S8, S9, S10). αTTP protein is considered to be involved in the intracellular transport of vitamin E in mammals (Manor and Morley 2007; Kono and Arai 2015). Retinal photoreceptors of mammals are known to express αTTP, and the supply of vitamin E is expected to contribute to the prevention of the oxidation of polyunsaturated fatty acids contained in the developed membranous structures of photoreceptors (Shichiri et al. 2012). However, it has not been demonstrated that the currently identified αTTP of *Limax* and *Peronia* actually functions as a transporter of α-tocopherol, although the overall amino acid sequences support the categorization of these proteins into the clade of αTTP (Fig. 1). Notably, recombinant human αTTP has been shown to weakly bind 9-*cis*-retinal, with a dissociation constant of 786 nM (Panagabko et al. 2003). Therefore, the endogenous ligand for αTTP in *Limax* and *Peronia* remains unclear. It is possible that these proteins substantially bind 11-*cis*-retinal in the photoreceptors where the concentration of retinal is expected to be high and may serve overlapping roles with RALBP and/or RLBP1.

Finally, we found that RALBP is present in the cornea of the tentacular eye of *Limax* and the SE of *Peronia*. The cornea of gastropod has been considered to contribute to the refraction of incident light and to the secretion of the material for lens formation (Kataoka 1977; Zieger & Mayer-Rochow 2008). The presence of RALBP (and also αTTP), but not retinochrome, is intriguing, and may suggest previously unappreciated roles of the cornea in the biochemistry of lipophilic compounds, independent of opsin-related functions. For example, an appropriate concentration of retinoids is important for the development and regeneration of corneal cells in humans (Samarawickrama et al. 2015), and RALBP may be involved in the adjustment of free retinoid concentration in the cell.

Collectively, our present study demonstrated that the RALBP-retinochrome system is not obligatory for all bistable opsin-based visual pigments in gastropods. Gq-rhodopsin-expressing cells invariably require this system in the same cells on one hand, whereas photosensors expressing only Opn5A or Xenopsin do not necessarily do so. This difference may be partly due to the difference in the absolute amountsof opsin molecules expressed in the photoreceptors (Matsuo et al. 2019; Nishiyama et al. 2019). The number of chromophores that failed to be regenerated by the bistability of opsins and detach from opsin would be so large that other regeneration systems are needed in such photoreceptors. Cell-autonomous regenerative system of retinal with RALBP-retinochrome may be an exquisite device for the supply of 11-*cis*-retinal to suffice the need from a large amount of Gq-rhodopsins in the highly developed rhabdomeric photoreceptors in mollusks.

Supplementary Information The online version contains supplementary material available at https://doi.org/10.1007/s00359-024-01712-7.

Acknowledgements This study was supported by a Grant from Nakatsuji Foresight Foundation (to RM).

Author contribution R.M. conceived the study. K.T. performed molecular phylogenetic analysis (Fig. 1). R.M. performed RT-PCR analysis, antibody generation, and histological experiments (Figs. 2–8, S1-14). H.K. performed antibody generation and histological experiments (Figs. S4, S10). Y.M. performed experiments using neurobiotin (Figs. 4, 5). T.N. collected animals and helped in antibody generation. R.M. wrote the manuscript. All authors reviewed the manuscript.

Data availability Accession numbers of the nucleotide sequence data and RRID for antibodies are provided within the manuscript file and Table S1.

Declarations

Conflict of interest The authors declare no competing interests.

References

Alvarez CE (2008) On the origins of arrestin and rhodopsin. BMC Ecol Evol 8:222

Bodington A (1890) Studies in evolution and biology. Elliot Stock, London

Brandenburger JL (1975) Two new kinds of retinal cells in the eye of a snail, *Helix aspersa*. J Ultrast Res 50:216–230

Capella-Gutiérrez S, Silla-Martínez JM, Gabaldón T (2009) trimAl: a tool for automated alignment trimming in large-scale phylogenetic analyses. Bioinformatics 25:1972–1973

Choi EH, Daruwalla A, Suh S, Leinone H, Palczewski K (2021) Retinoids in the visual cycle: role of the retinal G protein-coupled receptor. J Lipid Res 62:100040

Chomczynski P, Sacchi N (1987) Single-step method of RNA isolation by acid guanidinium thiocyanate-phenol-chloroform extraction. Anal Biochem 162:156–159

Crozier WJ, Arey LB (1919) The heliotropism of *Onchidium*: a problem in the analysis of animal conduct. J Gen Physiol 2:107–112

de Hoog E, Lukewich MK, Spencer GE (2019) Retinoid receptor-based signaling plays a role in voltage-dependent inhibition of invertebrate voltage-gated Ca^{2+} channels. J Biol Chem 294:10076–10093

Defoe DM, Bok D (1983) Rhodopsin chromophore exchanges among opsin molecules in the dark. Invest Ophthalmol vis Sci 24:1211–1226

DeWire SM, Ahn S, Lefkowitz RJ, Shenoy SK (2007) β-arrestin and cell signaling. Annu Rev Physiol 69:483–510

Döring CC, Kumar S, Tumu SC, Kourtesis I, Hausen H (2020) The visual pigment xenopsin is widespread in protostome eyes and impacts the view on eye evolution. eLife 9:e55193

Doyle SE, Castrucci AM, McCall M, Provencio I, Menaker M (2006) Nonvisual light responses in the Rpe65 knockout mouse: rod loss restores sensitivity to the melanopsin system. Proc Natl Acad Sci USA 103:10432–10437

Edgar RC (2004) MUSCLE: a multiple sequence alignment method with reduced time and space complexity. BMC Bioinform 5:113

Fukunaga S, Matsuo R, Hoshino S, Kirino Y (2006) Novel kruppel-like factor is induced by neuronal activity and by sensory input in the central nervous system of the terrestrial slug *Limax valentianus*. J Neurobiol 66:169–181

Gomez MP, Espinosa L, Ramirez N, Nasi E (2011) Arrestin in ciliary invertebrate photoreceptors: molecular identification and functional analysis in vivo. J Neurosci 31:1811–1819

Hara T, Hara R (1967) Rhodopsin and retinochrome in the squid retina. Nature 214:573–575

Hara T, Hara R (1973) Isomerization of retinal catalysed by retinochrome in the light. Nature 242:39–43

Hara T, Hara R (1980) Retinochrome and rhodopsin in the extraocular photoreceptor of squid, *Todarodes*. J Gen Physiol 75:1–19

Harrison KR, Reifler AN, Chervenak AP, Wong KY (2021) Prolonged melanopsin-based photoresponses depend in part on RPE65 and cellular retinaldehyde-binding protein (CRALBP). Curr Eye Res 46:515–523

Katagiri N (1984) Cytoplasmic characteristics of three different rhabdomeric photoreceptor cells in a marine gastropod, *Onchidium verruculatum*. Microscopy 33:142–150

Katagiri Y, Katagiri N, Fujimoto K (1985) Morphological and electrophysiological studies of a multiple photoreceptive system in a marine gastropod, *Onchidium*. Neurosi Res Supple 2:S1–S15

Katagiri N, Terakita A, Shichida Y, Katagiri Y (2001) Demonstration of a rhodopsin-retinochrome system in the stalk eye of a marine gastropod, *Onchidium*, by immunohistochemistry. J Comp Neurol 433:380–389

Katagiri N, Suzuki T, Shimatani Y, Katagiri Y (2002) Localization of retinal proteins in the stalk and dorsal eyes of the marine gastropod, *Onchidium*. Zool Sci 19:1231–1240

Kataoka S (1975) Fine structure of the retina of a slug, *Limax flavus* L. Vsion Res 15:681–686

Kataoka S (1977) Ultrastructure of the cornea and accessory retina in a slug, *Limax flavus* L. J Ultrast Res 60:296–305

Kojima D, Mori S, Torii M, Wada A, Morishita R, Fukada Y (2011) UV-sensitive photoreceptor protein Opn5 in humans and mice. PLoS ONE 6:e26388

Kono N, Arai H (2015) Intracellular transport of fat-soluble vitamins A and E. Traffic 16:19–34

Koyanagi M, Terakita A (2014) Diversity of animal opsin-based pigments and their optogenetic potential. Biochim Biophys Acta 1837:710–716

Maden M (2002) Retinoid signaling in the development of the central nervous system. Nat Rev Neurosci 3:843–853

Manor D, Morley S (2007) The alpha-tocopherol transfer protein. Vitam Horm 76:45–65

Matsumoto H, Tokunaga F, Yoshizawa T (1975) Accessibility of the iodopsin chromophore. Biochim Biophys Acta 404:300–308

Matsuo R, Matsuo Y (2022) Regional expression of neuropeptides in the retina of the terrestrial slug *Limax valentianus* (Gastropoda, Stylommatophora, Limacidae). J Comp Neurol 530:1551–1568

Matsuo R, Asada A, Fujitani K, Inokuchi K (2001) LIRF, a gene induced during hippocampal long-term potentiation as an immediate-early gene, encodes a novel RING finger protein. Biochem Biophys Res Commun 289:479–484

Matsuo Y, Uozumi N, Matsuo R (2014) Photo-tropotaxis based on projection through the cerebral commissure in the terrestrial slug *Limax*. J Comp Physiol A 200:1023–1032

Matsuo R, Takatori Y, Hamada S, Koyanagi M, Matsuo Y (2017) Expression and light-dependent translocation of β–arrestin in the visual system of the terrestrial slug *Limax valentianus*. J Exp Biol 220:3301–3314

Matsuo Y, Yamanaka A, Matsuo R (2018) RFamidergic neurons in the olfactory centers of the terrestrial slug *Limax*. Zoological Lett 4:22

Matsuo R, Koyanagi M, Nagata A, Matsuo Y (2019) Co-expression of opsins in the eye photoreceptor cells of the terrestrial slug *Limax valentianus*. J Comp Neurol 527:3073–3086

Matsuo Y, Nishiyama H, Matsuo R (2020) Integration of ocular and non-ocular photosensory information in the brain of the terrestrial slug *Limax*. J Comp Physiol A 206:907–919

Matsuo R, Kotoh S, Takishita K, Sakamoto K, Uebi T, Ozaki M, Matsuo Y, Nishi T (2022) Opsins in the cephalic and extracephalic photoreceptors in the marine gastropod *Onchidium verruculatum*. Biol Bull 243:339–352

Matsuo R, Koyanagi M, Sugihara T, Shirata T, Nagata T, Inoue K, Matsuo Y, Terakita A (2023) Functional characterization of four opsins and two G alpha subtypes co-expressed in the molluscan rhabdomeric photoreceptor. BMC Biol 21:291

Matsuo Y, Kawakami A, Matsuo R (2024) Visual afferents from an eye in the terrestrial slug *Limax valentianus*. J Comp Neurol 532:e25600

McCrohan CR, Benjamin PR (1980) Synaptic relationships of the cerebral giant cells with motoneurons in the feeding system of *Lymnaea stagnalis*. J Exp Biol 85:169–186

Minh BQ, Nguyen MA, von Haeseler A (2013) Ultrafast approximation for phylogenetic bootstrap. Mol Biol Evol 30:1188–1195

Moiseyev G, Chen Y, Takahashi Y, Wu BX, Ma J (2005) RPE65 is the isomerohydrolase in the retinoid visual cycle. Proc Natl Acad Sci USA 102:12413–12418

Molina TM, Torres SC, Flores A, Hara T, Hara R, Robles LJ (1992) Immunocytochemical localization of retinal binding protein in the octopus retina: a shuttle protein for 11-cis retinal. Exp Eye Res 54:83–90

Nakashima Y, Kusakabe T, Kusakabe R, Terakita A, Shichida Y, Tsuda M (2003) Origin of the vertebrate visual cycle: Genes encoding retinal photoisomerase and two putativevisual cycle proteins are expressed in whole brain of a primitive chordate. J Comp Neurol 460:180–190

Nguyen LT, Schmidt HA, von Haeseler A, Minh BG (2015) IQ-TREE: a fast and effective stochastic algorithm for estimating maximum-likelihood phylogenies. Mol Biol Evol 32:268–274

Nishiyama H, Nagata A, Matsuo Y, Matsuo R (2019) Light avoidance by a non-ocular photosensing system in the terrestrial slug *Limax velantianus*. J Exp Biol 222:jeb208595

Nobes C, Baverstock J, Saibil H (1992) Activation of the GTP-binding protein Gq by rhodopsin in squid photoreceptors. Biochem J 287:545–548

Ozaki K, Hara R, Hara T (1983) Histochemical localization of retinochrome and rhodopsin studied by fluorescence microscopy. Cell Tissue Res 233:335–345

Ozaki K, Terakita A, Hara R, Hara T (1987) Isolation and characterization of a retinal-binding protein from the squid retina. Vision Res 27:1057–1070

Ozaki K, Terakita A, Ozaki M, Hara R, Hara T, Hara-Nishimura I, Mori H, Nishimura M (1994) Molecular characterization and functional expression of squid retinal-binding protein. a novel

species of hydrophobic ligand-binding protein. J Biol Chem 269:3838–3845
Palczewski K, Kiser PD (2020) Shedding new light on the generation of the visual chromophore. Proc Natl Acad Sci USA 117:19629–19638
Panagabko C, Morley S, Hernandez M, Cassolato P, Gordon H, Parsons R, Manor D, Atkinson J (2003) Ligand specificity in the CRAL-TRIO protein family. Biochemistry 42:6467–6474
Robles LJ, Watanabe A, Kremer NE, Wong F, Bok D (1987) Immunocytochemical localization of photopigments in cephalopod retinae. J Neurocytol 16:403–415
Ronquist F, Huelsenbeck JP (2003) MrBayes 3: bayesian phylogenetic inference under mixed models. Bioinformatics 19:1572–1574
Saito K, Tautz L, Mustelin T (2007) The lipid-binding SEC14 domain. Biochim Biophys Acta 1771:719–726
Samarawickrama C, Chew S, Watson S (2015) Retinoic acid and the ocular surface. Surv Ophthalmol 60:183–195
Shen D, Jiang M, Hao W, Tao L, Salazar M, Fong HKW (1994) A human opsin-related gene that encodes a retinaldehyde-binding protein. Biochemistry 33:13117–13125
Shichiri M, Kono N, Shimanaka Y, Tanito M, Rotzoll DE, Yoshida Y, Hagihira Y, Tamai H, Arai H (2012) A novel role for α-tochopherol transfer protein (α-TTP) in protecting against chloroquine toxicity. J Biol Chem 287:2926–2934
Smith G, Briscoe A (2015) Molecular evolution and expression of the CRAL-TRIO protein family in insects. Insect Biochem Mol Biol 62:168–173
Terakita A, Hara R, Hara T (1989) Retinal-binding protein as a shuttle for retinal in the rhodopsin-retinochrome system of the squid visual cells. Vision Res 29:639–652
Tsuda M, Kusakabe T, Iwamoto H, Horie T, Nakashima Y, Nakagawa M, Okunou K (2003) Origin of the vertebrate visual cycle: II. Visual cycle proteins are localized in whole brain including photoreceptor cells of a primitive chordate. Vision Res 43:3045–3053
Tu DC, Owens LA, Anderson L, Golczak M, Doyle SE, McCall M, Menaker M, Palczewski K, Van Gelder R (2006) Inner retinal photoreception independent of the visual retinoid cycle. Proc Natl Acad Sci USA 103:10426–10431
Tworak A, Kolesnikov AV, Hong JD, Choi EH, Luu JC, Palczewska G, Dong Z, Lewandowski D, Brooks MJ, Campello L, Swaroop A, Kiser PD, Kefalov VJ, Palczewski K (2023) Rapid RGR-dependent visual pigment recycling is mediated by the RPE and specialized Müller glia. Cell Rep 42:112982
Vesprini ND, Dawson TF, Yuan Y, Bruce D, Spencer GE (2015) Retinoic acid affects calcium signaling in adult molluscan neurons. J Neurophysiol 113:172–181
Vöcking O, Leclère L, Hausen H (2021) The rhodopsin-retinochrome system for retinal re-isomerization predates the origin of cephalopod eyes. BMC Ecol Evol 21:215
Vöcking O, Kourtesis I, Tumu SC, Hausen H (2017) Co-expression of xenopsin and rhabdomeric opsin in photoreceptors bearing microvilli and cilia. eLife 6:e23435
von Lintig J, Moon J, Babino D (2021) Molecular components affecting carotenoid and retinoid homeostasis. Prog Retin Eye Res 80:100864
Weir J (1899) The dawn of reason. Macmillan, London
Wignrove J, de Hoog E, Spencer GE (2023) Disruptions in network plasticity precede deficits in memory following inhibition of retinoid signaling. J Neurophysiol 129:41–55
Yamashita T, Ohuchi H, Tomonari S, Ikeda K, Sakai K, Shichida Y (2010) Opn5 is a UV-sensitive bistable pigment that couples with Gi subtype of G protein. Proc Natl Acad Sci USA 107:22084–22089
Yanase T, Okuno Y, Uchida H (1981) Electrophysiological studies on the visual cell and lens cell of dorsal eye in *Onchidium verruculatum*. Mem Osaka Kyoiku Univ Ser III 29:121–126
Yeoman MS, Brierley MJ, Benjamin PR (1996) Central pattern generator interneurons are targets for the modulatory serotonergic cerebral giant cells in the feeding system of *Lymnaea*. J Neurophysiol 75:11–25
Yoshida MA, Ogura A, Ikeo K, Shigeno S, Moritaki T, Winters GC, Kohn AB, Moroz LL (2015) Molecular evidence for convergence and parallelism in evolution of complex brains of cephalopod molluscs: insights from visual systems. Integr Comp Biol 55:1070–1083
Zhang J, Choi EH, Tworak A, Salom D, Leinonen H, Sander CL, Hoang TV, Handa JT, Blackshaw S, Palczewska G, Kiser PD, Palczewski K (2019) Photic generation of 11-cis-retinal in bovine retinal pigment epithelium. J Biol Chem 294:19137–19154
Zhang Y, Mao F, Mu H, Huang M, Bao Y, Wang L, Wong NK, Xiao S, Dai H, Xiang Z, Ma M, Xiong Y, Zhang Z, Zhang L, Song X, Wang F, Mu X, Li J, Ma H, Zhang Y, Zheng H, Simakov O, Yu Z (2021) The genome of *Nautilus pompilius* illuminates eye evolution and biomineralization. Nat Ecol Evol 5:927–938
Zieger MV, Meyer-Rochow VB (2008) Understanding the cephalic eyes of pulmonate gastropods: a review. Am Malacol Bull 26:47–66